### ChemComm

## COMMUNICATION

# An octahedral coordination cage with six Fe(III) centers as a $T_1$ MRI probe

Aruni Dissanayake, <sup>a</sup> Joseph A. Spernyak <sup>b</sup> and Janet R. Morrow <sup>a</sup>

Received 00th January 20xx, Accepted 00th January 20xx

DOI: 10.1039/x0xx00000x

The incorporation of multiple Fe(III) centers bridged by rigid ligands into a coordination cage represents a powerful approach for designing effective MRI contrast agents. In this context, an octahedral coordination cage with six high-spin Fe(III) centers is shown to be water soluble, robust towards dissociation and has effective relaxivity as a  $T_1$  MRI probe in solution and in mice.

Self-assembled coordination cages show promise for the development of new classes of biomedical imaging probes.1 Coordination cages have rigid organic linkers connecting multiple metal ion centers to give symmetrical threedimensional shapes. The high degree of symmetry of these metal organic polyhedra may be advantageous for imaging applications that would benefit from increased signal intensity. As well-defined molecules, the properties of coordination cages may be tuned at a molecular level to produce responsive probes for molecular imaging. Coordination cages have been studied as MRI,<sup>2, 3</sup> radiopharmaceutical<sup>4, 5</sup> or fluorescent <sup>6, 7</sup> probes. The scaffold of a coordination cage may itself contain the imaging probe, such as paramagnetic or luminescent metal ions incorporated into the cage. Alternatively, the organic linkers may be further appended with recognition groups or additional imaging probes. Moreover, the container-like properties of coordination cages for the encapsulation of guest molecules are a unique feature with biomedical applications. Such host-guest properties are a further motivation for studying coordination cages as imaging or theranostic probes.

Our interest in coordination cages that contain biologically relevant metal ions for MR imaging applications<sup>8, 9</sup> have led us to study iron-based cages.<sup>2</sup> Iron MRI probes are of interest as alternatives to Gd(III) based agents and high-spin Fe(III) complexes are of particular interest as a biologically relevant metal that can be stored and recycled by the human body.<sup>10, 11</sup>

Additional examples of Fe(III) coordination cages with distinct polyhedral shapes and coordination spheres would add to our understanding of the factors that are important in the development of this new class of Fe(III) MRI probes. 15, 16 Here we show that an octahedral Fe(III) coordination cage with six Fe(III) centers connected through four linkers (L) and containing acylhydrazone linkages forms a compound with composition of K<sub>6</sub>[Fe<sub>6</sub>L<sub>4</sub>] as a high relaxivity MRI probe that is very inert to dissociation. These studies were motivated by a recent report of an octahedral Ga(III) cage with acylhydrazone linkages and sulfonated phenolate donor groups which is soluble in aqueous solution.17 Given that Ga(III) has an ionic radius and coordination sphere that is similar to that of Fe(III), we were inspired to study iron cages with this type of linker. The research described here is only the second example, to the best of our knowledge, of an iron coordination cage developed for use as a transition metal-based alternative to Ln(III) MRI probes.

The  $M_6L_4$  cages were prepared by combining four C3-symmetric facial linkers formed from tris-acylhydrazide and salicylaldehyde ( $H_6L$ ) and six  $M(acac)_3$  where M is Fe(III) or Ga(III) (Scheme 1). Each linker contains three tridentate ligands emanating from the central aromatic group. The three donor groups are the phenolate oxygen, and the nitrogen and oxygen donors of the acylhydrazone moiety.

The most commonly studied Fe(III) complexes for MRI contain macrocycles or linear chelators.  $^{8}$ ,  $^{12}$ ,  $^{13}$  In comparison, self-assembled iron coordination cages are a little explored but promising alternative approach to effective  $T_1$  MRI probes. Our initial example of coordination cages for MRI featured the self-assembled Fe(III) tetrahedral cages first reported by the Raymond group ( $K_{12}[Fe_4L_6]$ ) [L=N,N-bis(2,3-dihydroxybenzoyl)-1,5-diaminonaphthalene).  $^{14}$  These cages contain high spin Fe(III) centers  $^{2}$ ,  $^{14}$  and have the advantage of being kinetically robust towards dissociation in aqueous solution even when challenged with competing ligands such as EDTA. An added benefit is the effective proton relaxivity produced by the four tightly connected Fe(III) centers that tumble slowly in solution and the accumulation of the MRI probe in murine tumors.  $^{2}$ 

<sup>&</sup>lt;sup>a</sup> Department of Chemistry, University at Buffalo, The State University of New York, Amherst, NY 14260, United States

b. Department of Cell Stress Biology, Roswell Park Comprehensive Cancer Center, Buffalo, New York 14263, United States

Supplementary Information available: Experimental details, spectroscopic data, relaxivity plots and data of mice MRI studies available. See DOI: 10.1039/x0xx00000x

COMMUNICATION ChemComm

 $\textbf{Scheme 1}. \ \ \textbf{Synthesis of coordination cages and configurations about metal center}.$ 

In the proposed cage structure, each M(III) binds to two of the tridentate ligands to give a six-coordinate center as shown in Scheme 1. Analogous Fe(III) bis-hydrazone or bissemicarbazone complexes have been structurally characterized and shown to have six-coordinate centers.<sup>18</sup>

The diamagnetic K<sub>6</sub>[Ga<sub>6</sub>L<sub>4</sub>] cage was prepared initially to facilitate the use of NMR spectroscopy as a tool for characterization. The diamagnetic  $Ga_6L_4$  cage shows six proton resonances, consistent with a highly symmetrical octahedral structure. In this octahedron, all M(III) centers are sixcoordinate and bound to four oxygen donor atoms and two nitrogen donors. As noted previously for the Ga(III) cage with sulfonated phenols, there are two enantiomeric configurations of the metal center (M or P axial chirality) due to the two different arrangements of the asymmetric acylhydrazone chelate (Scheme 1).17 If each of the six Ga(III) centers independently assumed M or P to give a cage with mixed configurations, there would be many different isomers. The presence of the simple <sup>1</sup>H NMR spectrum is consistent with a symmetrical cage with homochiral Ga(III) centers that are enantiomeric and can be designated as M<sub>6</sub> or P<sub>6</sub>. The diffusion ordered spectroscopy (DOSY) plot for the Ga(III) cage is consistent with a cage radius of 1.55 nm (Figure S6) which compares to the sulfonated cage radius of 1.47 nm.<sup>17</sup> The composition of the Ga cage is further supported by high resolution mass spectrometry by electrospray ionization (HRMS-ESI) analysis. The m/z peaks that are observed at 885.0312 and 663.5220 are assigned to species with a -3 charged [Ga<sub>6</sub>L<sub>4</sub>+3H<sup>+</sup>]<sup>3-</sup> and -4 charged species [Ga<sub>6</sub>L<sub>4</sub>+2H<sup>+</sup>]<sup>4-</sup> with isotopic distribution patterns separated by 0.3334  $\pm\,0.0005$  and  $0.2501\pm0.0004$  dalton respectively (Figure S8 and S9).

The Fe(III) cage was prepared in a similar manner by addition of four equivalents of the linker, L, to six equivalents of Fe(acac) $_3$  to give Fe $_6$ L $_4$ . Analysis for iron is consistent with a formulation as K $_6$ [Fe $_6$ (L $_4$ )] which suggests that all acylhydrazones and phenol groups are fully deprotonated upon isolation of the coordination cage. Studies on bis-acylhydrazone complexes of Fe(III) also feature deprotonated acylhydrazone linkages. <sup>18, 19</sup> A coordination cage with four fully deprotonated linkers and six trivalent metal ions would have an overall charge of negative six

in solution. The ESI-HRMS spectrum of  $K_6[Fe_6L_4]$  demonstrates intense peaks at m/z= 857.3848 and 642.7872 which are assigned to  $[Fe_6L_4+3H^+]^{3-}$  and  $[Fe_6L_4+2H^+]^{4-}$  respectively. Isotopic distribution patterns observed for the above predominant peaks follow the simulated patterns obtained based on the natural isotopic abundances (Figures 1 and S11).

The solution chemistry of the iron coordination cage was studied prior to investigation of the cage as an MRI probe. The water solubility of the iron-based cage is approximately 500  $\mu M$ at neutral pH in PBS buffer. However, 1 mM concentrations were obtained in the presence of excess meglumine, a common additive for MRI contrast agents. The electronic absorbance spectroscopy of the iron cage in water shows a ligand to metal charge transfer (LMCT) band and several acylhydrazone-based absorbances in the UV region (Figs S12-S17). Monitoring of the LMCT band over time showed that the iron coordination cage stayed intact in phosphate saline buffer over 4 hours at neutral pH. Moreover, the kinetic inertness of the cage was challenged in the presence of a 10-fold excess of Zn(II) at 37 °C. The constancy of the LMCT band (Figure S15) is consistent with the absence of trans-metalation of the cage. Incubation of the iron coordination cage with an equivalent of EDTA also did not lead to disruption of the cage. Finally, incubation of the cage with transferrin with monitoring by UV-vis spectroscopy suggests that the cage is robust towards loss of iron to this iron storage protein.

Further characterization of the iron cage in aqueous solution shows that the Fe(III) centers are in high-spin state and stabilized as trivalent iron. Solution magnetic susceptibility measurements by Evans method gives an effective magnetic moment of 5.6 per iron, supporting high-spin Fe(III) (Figure S18). The <sup>1</sup>H NMR of the iron complex shows an absence of <sup>1</sup>H resonances, which is consistent with a high-spin paramagnetic center (Figure S19). Cyclic voltammetry studies are consistent with a stabilized trivalent Fe(III) center. The redox potential of -0.83 V versus NHE is sufficiently negative to maintain the trivalent state under biological conditions. <sup>8, 20</sup>

Relaxometry studies to measure longitudinal  $(T_1)$  or transverse  $(T_2)$  relaxation of bulk water protons in the presence of the iron cage support the presence of high-spin Fe(III) centers. These centers increase proton relaxation rates  $(R_1$  and  $R_2)$  which are normalized to 1 mM Fe(III) and are reported as  $r_1$  and  $r_2$  relaxivities.

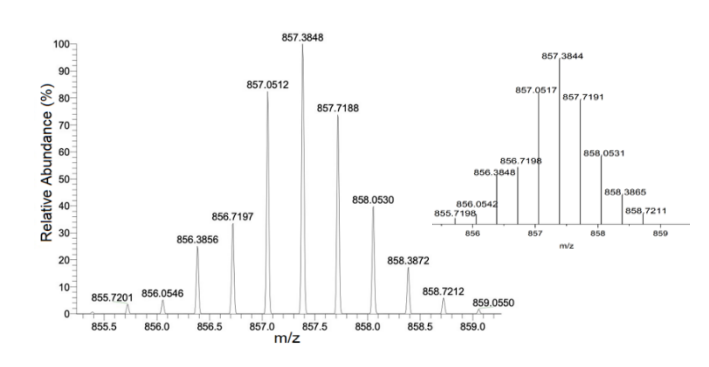


**Figure 1.** HRMS-ESI of Fe<sub>6</sub>L<sub>4</sub> showing observed isotopic distribution pattern for m/Z = 3-([Fe<sub>6</sub>L<sub>4</sub>+3H<sup>+</sup>]<sup>3-</sup>) and theoretical isotope pattern as the insert.

Journal Name COMMUNICATION

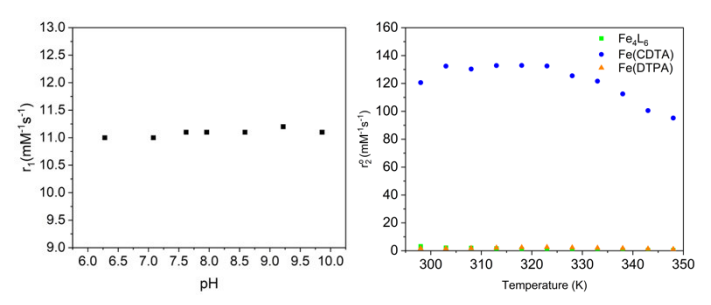


**Figure 2.** The pH dependence of  $r_1$  relaxivity of Fe<sub>6</sub>L<sub>4</sub> in PBS buffer at 1.4 T, 34 °C (left). Comparison of  $^{17}$ O NMR transverse relaxivity ( $r_2$ ° per iron) for Fe<sub>6</sub>L<sub>4</sub> at pH 7.5, Fe(CDTA) at pH 6.8, and Fe(DTPA) at pH 6.8 as a function of temperature (right).

The acyl hydrazone cage (Fe<sub>6</sub>L<sub>4</sub>) had a r<sub>1</sub> relaxivity of 11 mM<sup>-1</sup> <sup>1</sup>s<sup>-1</sup> per cage (1.8 mM<sup>-1</sup>s<sup>-1</sup> per Fe) at 1.4 T and 34 °C, pH 7.4 in PBS buffer, whereas the Raymond cage has a r<sub>1</sub> of 8.4 mM<sup>-1</sup>s<sup>-1</sup> per cage (2.1 mM<sup>-1</sup>s<sup>-1</sup> per Fe) and the mononuclear complex<sup>21</sup>, Fe(PTOB), is 0.98 mM<sup>-1</sup>s<sup>-1</sup>. These data are best understood through consideration of relaxation theory.<sup>22</sup> Proton relaxation by paramagnetic iron centers is mediated by interaction with water molecules, predominantly through magnetic dipolar interactions.<sup>15, 22</sup> Water molecules may be directly bound (IS, inner-sphere), associated with ligands (SS, second-sphere) or closely diffusing (OS, outer-sphere) with respect to the iron center. Dipolar coupling between paramagnetic center and water protons is modulated by correlation times including those involving electronic relaxation ( $\tau_{1e}$ ), water exchange ( $\tau_{m}$ ) and rotational motion ( $\tau_R$ ). Notably, the Fe(III) complexes listed in Table 1 lack an inner-sphere water molecule as shown by variable temperature <sup>17</sup>O NMR studies.<sup>2,21</sup> Analogous studies on  $Fe_6L_4$  (Fig 2) suggest that the transverse  $^{17}O$  relaxation  $r_2{}^O$  is similar to that of Fe(DTPA), which lacks an IS water rather than to Fe(CDTA) with an exchangeable IS water (Figure 2).

The r<sub>1</sub> relaxivity of the coordination cages is remarkably high per iron center for a probe that acts through SS or OS water only. In comparison, the mononuclear complex, Fe(PTOB), has a  $r_1$  of approximately 1 mM-1s-1, which is typical for closed coordination Fe(III) centers.8, 12 An important contributing factor is undoubtably the larger size of the cages and the correspondingly slower rotational tumbling as represented by  $\tau_R$ . Rigid multimeric paramagnetic chelates are predicted to produce optimal  $T_1$  probes at 1.5-9.4 T.<sup>23</sup> To further probe the mechanism of water proton relaxation by Fe<sub>6</sub>L<sub>4</sub>,<sup>22</sup> the pH dependence of r<sub>1</sub> was studied (Figure 2). A pH dependence is observed if proton catalyzed relaxation of water molecules is an important mechanism<sup>24, 25</sup> or if there is a change in speciation due to ionization of the complex over the pH range. 16, 26 The lack of pH dependence of r<sub>1</sub> suggests that SS water interactions rather than proton exchange are operative and no speciation changes occur over this pH range. These data are congruent with other anionic Fe(III) complexes with phenolate groups that have strong SS water interactions.<sup>26</sup>

The  $r_1$  of the Fe<sub>6</sub>L<sub>4</sub> cage increases to 18 mM<sup>-1</sup>s<sup>-1</sup> upon addition of human serum albumin (HSA, 0.6 mM). This increase is consistent with binding of the coordination cage to serum albumin and the resultant slowing of the rotational motion of

the probe. Monitoring  $r_1$  as a function of HSA gives a binding isotherm that can be fit to a 4:1 stoichiometry (cage to protein)

Table 1. Water proton relaxivity values for Fe(III) complexes<sup>a</sup>

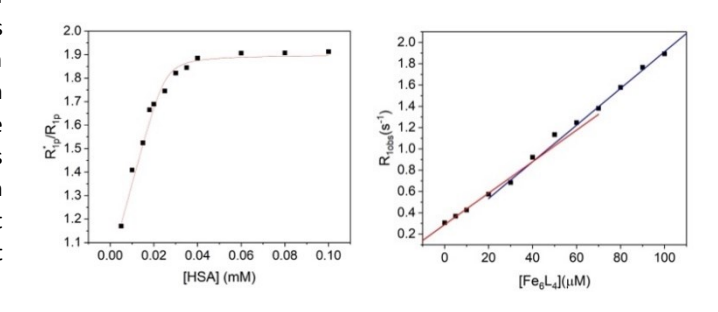
Complex	r <sub>1</sub> (mM <sup>-1</sup> s <sup>-1</sup> )	r₁ (mM <sup>-1</sup> s <sup>-1</sup> ) with HSA	r <sub>2</sub> (mM <sup>-1</sup> s <sup>-1</sup> )
Fe <sub>6</sub> L <sub>4</sub>	$\textbf{11.1} \pm \textbf{0.3}$	$\textbf{18.0} \pm \textbf{0.2}$	$14.7{\pm}\ 1.0$
	(1.8 per Fe)	(3.0 per Fe)	(2.4 per Fe)
Fe <sub>4</sub> A <sub>6</sub> <sup>b</sup>	$8.3 \pm 0.3$	$\textbf{26} \pm \textbf{0.1}$	-
	(2.1 per Fe)	(6.5 per Fe)	
Fe(PTOB) <sup>c</sup>	$\boldsymbol{0.98 \pm 0.05}$	$\textbf{1.4} \pm \textbf{0.07}$	$\textbf{1.2} \pm \textbf{0.2}$

 $^a$  Measured at pH 7.4, 1.4 T, 34 °C.  $^b$  reference 2,  $^c$  reference  $^{21}$  where PTOB is (2S,2'S)-1,1'-(7-(2-hydroxybenzyl)-1,4,7-triazonane-1,4-diyl)bis(propan-2-ol).

with an average association constant ( $K_a$ ) of 5.4 x 10<sup>5</sup> M<sup>-1</sup> (Eq S5-7, E plot). The M plot shows a break at a 4:1 ratio of cage to HSA, which supports the proposed stoichiometry (Figure 3).<sup>27</sup> In our case, the data fitting gives a lower limit for  $K_a$  as the binding isotherm is quite steep and the concentrations of cage probe must be in micromolar range for these measurements.

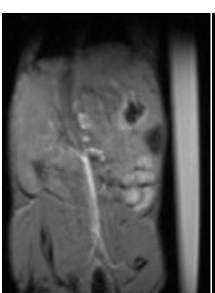
To further explore the mode of binding to HSA, the relaxivity of the iron coordination cage was studied in the presence of probes that are known to bind to the hydrophobic pockets of the serum protein including ibuprofen, iodipamide, methyl orange, warfarin or 1,3,6-trisulfonic acid (HTPS).<sup>28</sup> None of these competitive binders at 0.6 mM produced a change in the relaxivity of the cage, consistent with binding being predominantly electrostatic in nature.<sup>28</sup> However, it is possible that the competitive binders, although present in 8-fold excess, cannot effectively compete with the cage for serum albumin binding pockets. To further test for electrostatic interactions, the relaxivity of the cage was tested upon addition of poly-Llysine, a protein of cationic charge. The relaxivity increase from 11 mM<sup>-1</sup>s<sup>-1</sup> to 13 mM<sup>-1</sup>s<sup>-1</sup> suggests that electrostatic interactions contribute to binding of the MRI probe.

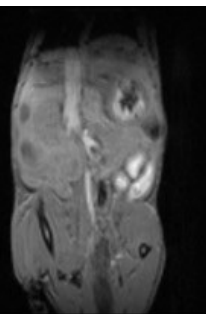
The Fe $_6L_4$  cage was injected into BALB/c mice at 10  $\mu$ mol/kg cage (60  $\mu$ mol iron/kg) and monitored by T $_1$  weighted MRI studies over 5-50 minutes (Figures 4 and S25-S27). There is enhanced contrast in the vena cava over this period suggesting that the cage acts as a blood pool agent, which is consistent with its strong binding to serum albumin.

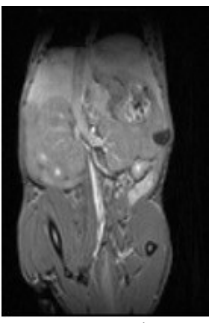


**Figure 3.** E (left) and M (right) titrations of enhancement factor versus HSA concentration and observed relaxation rate constants as a function of cage concentration, respectively. For E titration, 100  $\mu$ M Fe<sub>6</sub>L<sub>4</sub> in PBS (pH 7.4) and for M titration, 10  $\mu$ M HSA in PBS (pH 7.4) was used.

COMMUNICATION ChemComm







 $\label{eq:Figure 4.7} \textbf{Figure 4.} \ T_1\text{-weighted MR images of BALB/c mice upon injection of 10 $\mu$mol/kg cage $Fe_6L_4$.} \\ Vascular enhancement is observed from pre-injection (left) to 50-minute post-injection (right). MR image collected at 5-minute post-injection is at the middle.$ 

Pharmacokinetic clearance is mostly through the hepatobiliary system as shown by the enhanced contrast in liver compared to bladder over time (Figures S25-28). Analogous data for gadoterate meglumine is shown at 50  $\mu$ mol/kg to clearly visualize the differences between the blood pool behavior of the iron coordination cage in comparison to gadoterate as an example of a hydrophilic extracellular matrix contrast agent.

In summary, an octahedral Fe(III) cage has been prepared as one of the first examples of an effective T<sub>1</sub> MRI probe based on a self-assembled coordination cage. The combination of four oxygen donors and two nitrogen donors in the acylhydrazone framework stabilizes high-spin Fe(III) centers in the trivalent state to give a cage which is remarkably inert towards phosphate anions, EDTA, Zn(II) or transferrin. The high relaxivity of the coordination cage as shown by a r<sub>1</sub> of 1.8 mM<sup>-1</sup>s<sup>-1</sup> for each Fe(III) center or 11 mM<sup>-1</sup>s<sup>-1</sup> per molecule demonstrates the power of this approach. Coordination cages are especially promising for the development of high relaxivity probes based on Fe(III) because this approach makes it feasible to produce high relaxivity probes without requisite inner-sphere water ligands. Fe(III) complexes with inner-sphere water ligands often ionize to form hydroxide or bridging oxide ligands with a concomitant decrease in the relaxivity of the probe. 16

JRM thanks the NSF (CHE-2400128) for support of this work. J.A.S. is partially supported by Roswell Park's NIH P30 grant (CA016056). This work utilized a Bruker 500 MHz NMR (NSF CHE-2018160), ICP-MS and FTMS (NSF CHE-0959565).

A. Dissanayake: data curation, writing, analysis. J. Spernyak: writing, data curation and analysis. J. Morrow: writing, methodology, supervision, project administration.

#### **Conflicts of interest**

JRM is a cofounder of Ferric Contrast, a company that develops iron-based contrast agents.

#### Data availability

The data supporting this article have been included in the main article and as part of the supporting information.

#### References

(1) Moreno-Alcantar, G.; Casini, A. FEBS Lett 2023, 597, 191-202.

- (2) Sokolow, G. E.; Crawley, M. R.; Morphet, D. R.; Asik, D.; Spernyak, J. A.; McGray, A. J. R.; Cook, T. R.; Morrow, J. R. *Inorg Chem* **2022**, *61*, 2603-2611.
- (3) He, C.; Wu, X.; Kong, J. C.; Liu, T.; Zhang, X. L.; Duan, C. Y. *Chem Commun* **2012**, *48*, 9290-9292.
- (4) Woods, B.; Silva, R. D. M.; Schmidt, C.; Wragg, D.; Cavaco, M.; Neves, V.; Ferreira, V. F. C.; Gano, L.; Morais, T. S.; Mendes, F.; et al. *Bioconjuq Chem* **2021**, *32*, 1399-1408.
- (5) Burke, B. P.; Grantham, W.; Burke, M. J.; Nichol, G. S.; Roberts, D.; Renard, I.; Hargreaves, R.; Cawthorne, C.; Archibald, S. J.; Lusby, P. J. *J Am Chem Soc* **2018**, *140*, 16877-16881.
- (6) Qin, Y.; Chen, X.; Gui, Y.; Wang, H.; Tang, B. Z.; Wang, D. *J Am Chem Soc* **2022**, *144*, 12825-12833.
- (7) Zava, O.; Mattsson, J.; Therrien, B.; Dyson, P. J. *Chem-Eur J* **2010**, *16*, 1428-1431.
- (8) Kras, E. A.; Snyder, E. M.; Sokolow, G. E.; Morrow, J. R. *Acc. Chem. Res.* **2022**, *55*, 1435-1444.
- (9) Morrow, J. R.; Raymond, J. J.; Chowdhury, M. S. I.; Sahoo, P. R. *Inorg Chem* **2022**, *61* (37), 14487-14499.
- (10) Theil, E. C. Inorg Chem 2013, 52, 12223-12233.
- (11) Sargun, A.; Fisher, A. L.; Wolock, A. S.; Phillips, S.; Sojoodi, M.; Khanna, S.; Babitt, J. L.; Gale, E. M. *J Am Chem Soc* **2023**, *145*, 6871-6879.
- (12) Kuźnik, N.; Wyskocka, M. Eur J Inorg Chem **2016**, 2016, 445-458
- (13) Gupta, A.; Caravan, P.; Price, W. S.; Platas-Iglesias, C.; Gale, E. M. *Inorg Chem* **2020**, *59*, 6648-6678.
- (14) Caulder, D. L.; Bruckner, C.; Powers, R. E.; Konig, S.; Parac, T. N.; Leary, J. A.; Raymond, K. N. *J Am Chem Soc* **2001**, *123*, 8923-8938.
- (15) Baranyai, Z.; Carniato, F.; Nucera, A.; Horvath, D.; Tei, L.; Platas-Iglesias, C.; Botta, M. *Chem. Sci.* **2021**, *12*, 11138-11145.
- (16) Uzal-Varela, R.; Lucio-Martinez, F.; Nucera, A.; Botta, M.; Esteban-Gomez, D.; Valencia, L.; Rodriguez-Rodriguez, A.; Platas-Iglesias, C. *Inorg Chem Front* **2023**, *10* (5), 1633-1649.
- (17) Wu, G.; Chen, Y.; Fang, S.; Tong, L.; Shen, L.; Ge, C.; Pan, Y.; Shi, X.; Li, H. *Angew Chem Int Ed Engl* **2021**, *60*, 16594-16599.
- (18) Palanimuthu, D.; Wu, Z. X.; Jansson, P. J.; Braidy, N.; Bernhardt, P. V.; Richardson, D. R.; Kalinowski, D. S. *Dalton Trans* **2018**, *47*, 7190-7205.
- (19) Yu, J. X.; Kodibagkar, V. D.; Liu, L.; Zhang, Z. W.; Liu, L.; Magnusson, J.; Liu, Y. T. *Chem Sci* **2013**, *4*, 2132-2142.
- (20) Kosman, D. J. J Biol Chem 2010, 285, 26729-26735.
- (21) Kras, E. A.; Cineus, R.; Crawley, M. R.; Morrow, J. R. *Dalton Trans* **2024**, *53*, 4154-4164.
- (22) Wahsner, J.; Gale, E. M.; Rodriguez-Rodriguez, A.; Caravan, P. *Chem Rev* **2019**, *119*, 957-1057.
- (23) Caravan, P.; Farrar, C. T.; Frullano, L.; Uppal, R. *Contrast Media Mol Imaging* **2009**, *4*, 89-100.
- (24) Boccalon, M.; Leone, L.; Marino, G.; Demitri, N.; Baranyai, Z.; Tei, L. *Inorg Chem* **2021**, *60*, 13626-13636.
- (25) Carnovale, I. M.; Lolli, M. L.; Serra, S. C.; Mingo, A. F.; Napolitano, R.; Boi, V.; Guidolin, N.; Lattuada, L.; Tedoldi, F.; Baranyai, Z. *Chem Commun* **2018**, *54*, 10056-10059.
- (26) Nucera, A.; Carniato, F.; Baranyai, Z.; Platas-Iglesias, C.; Botta, M. *Inorg Chem* **2023**, *62*, 4272-4283.
- (27) Aime, S.; Botta, M.; Fasano, M.; Crich, S. G.; Terreno, E. *J Biol Inorg Chem* **1996**, *1*, 312-319.
- (28) Stefania, R.; Palagi, L.; Di Gregorio, E.; Ferrauto, G.; Dinatale, V.; Aime, S.; Gianolio, E. *J Am Chem Soc* **2023**, *146*, 134-144.